
Simple Steps to Success: Axiomatics of Distance-Based Algorithmic Recourse

Jenny Hamer
Google Research
hamer@google.com

Jake Valladares
University of Massachusetts, Amherst
jasonvallada@umass.edu

Vignesh Viswanathan
University of Massachusetts, Amherst
vviswanathan@umass.edu

Yair Zick
University of Massachusetts, Amherst
yzick@umass.edu

Abstract

We propose a novel data-driven framework for algorithmic recourse that offers users interventions to change their predicted outcome. Existing approaches to compute recourse find a set of points that satisfy some desiderata — e.g. an intervention in the underlying causal graph, or minimizing a cost function. Satisfying these criteria, however, requires extensive knowledge of the underlying model structure, often an unrealistic amount of information in several domains. We propose a data-driven, computationally efficient approach to computing algorithmic recourse. We do so by suggesting directions in the data manifold that users can take to change their predicted outcome. We present Stepwise Explainable Paths (StEP), an axiomatically justified framework to compute direction-based algorithmic recourse. We offer a thorough empirical and theoretical investigation of StEP. StEP offers provable privacy and robustness guarantees, and outperforms the state-of-the-art on several established recourse desiderata.

1 Introduction

An automatic decision maker produces a negative prediction for some user — e.g. denies their grad school application, offers them bad loan terms or an overly strict criminal sentence; what can the user do to change this outcome? Algorithmic recourse recommends actions that will change algorithmic predictions on a given point. This is usually modeled as a constrained optimization problem that outputs specific points which satisfy certain desirable properties: validity, data manifold closeness and causality to name a few. Such an approach may have some issues: it requires significant computing power and a significant amount of information. In this work, we propose a new method for algorithmic recourse; rather than searching for good interventions for users, we search for good *directions* that users can take. We use these directions to create an iterative recourse mechanism where stakeholders can repeatedly request new directions after carrying out the recommended changes. We show that by carefully choosing these directions, we can satisfy several desirable properties of algorithmic recourse at a significantly lower computational cost.

1.1 Our Contributions

We propose a family of directions for recourse called *Stepwise Explainable Paths* (StEP). Our key theoretical insight is that StEP is the *only method* for generating recourse directions which satisfies a set of natural properties. StEP directions are model agnostic and easy to compute, requiring only the training dataset and the output of the model of interest on points in the training dataset. That is,

Preprint. Under review.

our method does not require prior knowledge of the underlying model structure; in this, we take a strongly data-dependent approach. To summarize, our main contributions are

- (a) a novel Stepwise Explainable Path (StEP) based recourse framework, with provable quality (Section 3.1), diversity (Section 3.2) and privacy (Section 3.3) guarantees.
- (b) an extensive experimental evaluation of StEP, including a comparison to two state-of-the-art recourse methods, DiCE [Mothilal et al., 2020a] and FACE [Poyiadzi et al., 2020] on two financial datasets — the Credit Card Default [Yeh and Lien, 2009] and the Give Me Some Credit [Credit Fusion, 2011] datasets.

1.2 Related Work

Algorithmic recourse is a fundamental concept in the model explanation literature [Verma et al., 2020]. First proposed by Wachter et al. [2017], it has foundations in legal interpretations of explainability [Wachter et al., 2018] and is distinct from *feature highlighting* methods [Barocas et al., 2020], such as Shapley value-based methods [Datta et al., 2016, Lundberg and Lee, 2017], Local Interpretable Model-Agnostic Explanations (LIME) [Ribeiro et al., 2016] and saliency maps [Simonyan et al., 2013]. Whereas feature highlighting methods indicate important features (or feature interactions [Patel et al., 2021]), algorithmic recourse methods identify *changes* to features that would likely result in a different outcome. Most work on algorithmic recourse proposes the use of counterfactual explanations to recommend actions for stakeholders to take [Karimi et al., 2022, Verma et al., 2020]. These explanations are usually solutions to an optimization problem, ensuring that the explanations are valid, actionable, sparse and diverse [Mothilal et al., 2020a, Karimi et al., 2020a, Ustun et al., 2019]. The solutions to these optimization problems are computed using integer linear programs [Ustun et al., 2019, Kanamori et al., 2020], SAT solvers [Karimi et al., 2020a] or gradient descent [Mothilal et al., 2020a, Wachter et al., 2017]. Recent work provides a sequence of steps from the point of interest to a point with the desirable outcome along the data manifold [Poyiadzi et al., 2020]. While these prior methods offer reasonable approaches to recourse generation, none of them axiomatically characterize their approach.

Other work reformulates the problem of recommending actions as the causal problem of finding the best intervention [Karimi et al., 2021]. Karimi et al. [2021] argue that any recourse recommendation must be consistent with the underlying causal relations between variables. However, this requires complete (or, as in Karimi et al. [2020b], imperfect) knowledge of the underlying causal model, which is either unreasonable or computationally infeasible in many cases. Our work addresses this issue by providing users with promising directional actions; this allows stakeholders to flexibly choose what they do.

Our axiomatic approach is technically similar to the characterization of Monotone Influence Measures (MIM) [Sliwinski et al., 2019]. Sliwinski et al. [2019] propose a data-driven direction-based model explanation; however, their approach is not iterative in nature, nor is their recommended direction guaranteed to change the prediction outcome.

2 Preliminaries

We introduce some general notation, definitions used throughout this work and the setting of data-driven recourse. We denote by $\vec{x} \in \mathbb{R}^m$ a *point of interest* (PoI) and define a dataset $\mathcal{X} = \{\vec{x}^1, \vec{x}^2, \dots, \vec{x}^n\} \subseteq \mathbb{R}^m$ with m features and n datapoints. We use x_i to denote the i -th index of vector i .

Our setting centers on binary classification using a *model of interest* $f : \mathbb{R}^m \mapsto \pm 1$ trained on the dataset \mathcal{X} , where the goal is to provide recourse for $\vec{x} \notin \mathcal{X}$ such that $f(\vec{x}) = -1$. The *recourse* for a point of interest \vec{x} is a direction (or a set of directions) $\vec{d} \in \mathbb{R}^m$ that moves the point \vec{x} closer to the positive class, i.e. $f(\vec{x} + c \cdot \vec{d}) = 1$ for some positive value $c > 0$. Upon applying recourse to a PoI \vec{x} , we refer to $\vec{x} + c \cdot \vec{d}$ as a *counterfactual* (CF) of \vec{x} denoted by \vec{x}_{CF} .

Offering a user or stakeholder recourse only once may not be helpful; a given user may be unable to make a single dramatic change to their features or may not exactly follow the suggested recourse. We can allow the stakeholder to repeatedly request new recourse directions as they change their values

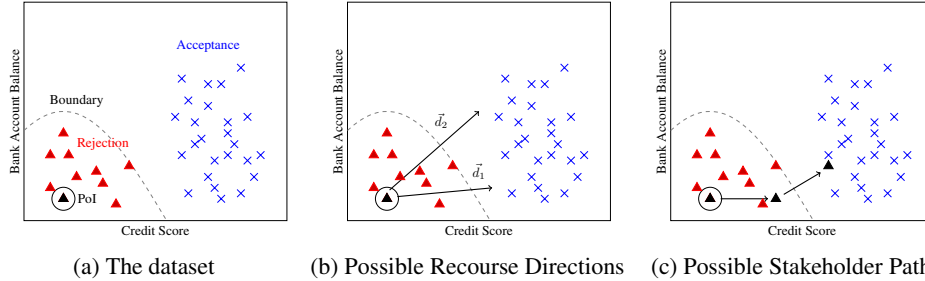


Figure 1: (Left) The training dataset that the loan approval algorithm uses, (Middle) Plotting possible recourse directions for Example 2.1 and (Right) plotting a stakeholder path toward loan acceptance.

until they are positively classified. We call such an approach *direction-based recourse*. To illustrate how this would work in practice, consider the following example of algorithmic loan approval.

Example 2.1. Consider a loan applicant whose application is rejected by a loan approval algorithm utilizing two factors: bank account balance and credit score. The loan applicant (i.e. the PoI), the algorithm and the training dataset are described in Figure 1a. Several directions could possibly change the PoI’s value from \triangle (red points with label -1) to \times (blue points with label $+1$). For example, increasing the credit score while leaving the bank account balance unchanged would ultimately shift the applicant’s label. Alternatively, increasing both the bank account balance and credit score (Figure 1b) would result in a positive outcome. Suppose that we provide the applicant with both alternatives; the applicant makes some modifications and reapplies for a loan. If the application is rejected again, we can provide them with new directions, given the applicant’s current state. We repeat this until the application is accepted. This results in a recourse *path*, rather than a single direction (see Figure 1c).

We wish to ensure that our directions are robust; thus, even if the stakeholder somewhat deviates from our suggested path, they are still likely to secure a positive outcome. This also “offloads” some of the computational costs onto the stakeholder, which guarantees certain recourse properties that would otherwise require a significant amount of information and computational cost. Consider Example 2.1: after providing two different directions, the change that the applicant makes to their data point will likely be a minimum cost change that approximately follows one of the directions we propose in Figure 1b. Even if the resulting change does not facilitate a change in outcome, or is incorrectly executed, we can still offer additional directions until a desirable outcome is obtained.

2.1 Data-driven Recourse

We propose a data driven approach to compute directions for recourse. Whether explanations should be computed based on the underlying model or the observed data is a highly debated topic [Chen et al., 2020, Barocas et al., 2020, Janzing et al., 2020]. While data-driven recourse methods exist (e.g. Poyiadzi et al. [2020]), most work solely with the model of interest f and search for a minimum distance intervention [Mothilal et al., 2020a, Wachter et al., 2017, Karimi et al., 2020a].

Recent work shows that explanations can perform poorly when they are inconsistent with the data manifold — i.e. the underlying distribution from which the data is drawn [Frye et al., 2021, Aas et al., 2021] and are vulnerable to manipulation [Slack et al., 2020, 2021]. We believe the effect of ignoring the data manifold when computing recourse could be even more pernicious, resulting in recourse recommendations that may not improve the outcome in any way, but simply move it outside the data manifold. To see why this is the case, consider Example 2.1 but with a different point of interest (given in Figure 2a). The shortest distance perturbation which crosses the decision boundary corresponds to the direction \vec{d}_1 (as given in Figure 2b). This direction suggests that the stakeholder decrease their credit score and marginally increase their bank account balance — a poor recourse recommendation since it actively moves the stakeholder away from the positively classified points. A recourse computing algorithm that recognizes the data manifold will offer a direction similar to \vec{d}_2 — a direction which arguably makes the stakeholder a better candidate for loan approval.

The above example has been deliberately simplified. One could argue that the model we choose (Figure 2) is oddly lenient when accepting loans; a more realistic model would be a simple hyperplane separating the two classes of data. However, when training complex models on complex datasets, it

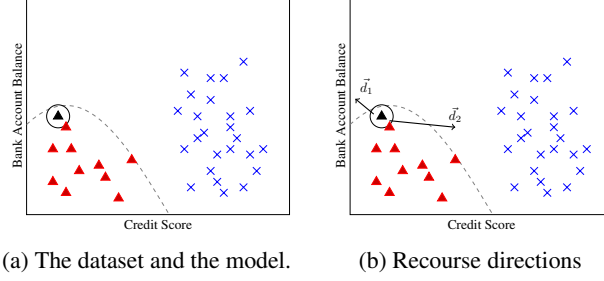


Figure 2: (Left) The training dataset that the loan approval algorithm uses, and (Right) Off manifold (\vec{d}_1) and On manifold (\vec{d}_2) directions.

Algorithm 1 The StEP Framework

Require: Dataset \mathcal{X} partitioned into k clusters $\{\mathcal{X}_1, \dots, \mathcal{X}_k\}$, point of interest \vec{x} , model f , some non-negatively valued function $\alpha : \mathbb{R}_{\geq 0} \mapsto \mathbb{R}_{\geq 0}$

- 1: **while** $f(\vec{x}) = -1$ **do**
- 2: **for** every cluster $c \in [k]$ **do** ▷ Generate a direction \vec{d}_c for every cluster c
- 3: $\vec{d}_c \leftarrow \sum_{\vec{x}' \in \mathcal{X}_c} (\vec{x}' - \vec{x}) \alpha(\|\vec{x}' - \vec{x}\|) \mathbb{1}(f(\vec{x}') = 1)$
- 4: **end for**
- 5: Offer the directions $\{d_c\}_{c \in [k]}$ to the stakeholder
- 6: Stakeholder returns an updated point of interest \vec{x}^*
- 7: $\vec{x} \leftarrow \vec{x}^*$
- 8: **end while**

is a very challenging task to determine model behavior on points outside the data manifold and the shape of the decision boundary. In such cases, it is a very real possibility that the decision boundary exhibits pathologies such as those shown in Figure 2a. Indeed, we observe this behavior in our experiments as well; in a credit card default prediction task [Yeh and Lien, 2009], we found that DiCE [Mothilal et al., 2020a] — a popular model-driven recourse generator — sometimes recommends paying a negative amount of money to reduce the chance of a credit default (see Appendix C.2).

3 Stepwise Explainable Paths (StEP)

We now present our approach to compute recourse directions. The overall framework is summarized in Algorithm 1. We first partition the dataset \mathcal{X} into k clusters $\{\mathcal{X}_1, \dots, \mathcal{X}_k\}$ (using a standard clustering algorithm). Then, for a point of interest \vec{x} , generate a direction \vec{d}_c towards each cluster c using the following expression

$$\vec{d}_c = \sum_{\vec{x}' \in \mathcal{X}_c} (\vec{x}' - \vec{x}) \alpha(\|\vec{x}' - \vec{x}\|) \mathbb{1}(f(\vec{x}') = 1) \quad (1)$$

where $\alpha : \mathbb{R}_+ \rightarrow \mathbb{R}_+$ is some non-negative function and $\|\cdot\|$ is a rotation invariant distance metric. We select directions using Equation (1) (a similar formula is proposed by Sliwinski et al. [2019]). The intuition behind this equation is as follows: for each point \vec{x}' in the cluster \mathcal{X}_c , if $f(\vec{x}') = 1$, we ‘move’ on the line $(\vec{x} - \vec{x}')$ a distance of $\alpha(\|\vec{x}' - \vec{x}\|)$, where α is a decreasing function of $\|\vec{x} - \vec{x}'\|$. Thus, points that are closer to \vec{x} will have a greater effect on \vec{d}_c ; similarly, several nearby positively classified points will have a greater effect on \vec{d}_c . We offer these k directions to the stakeholder, who then returns with a new point \vec{x}' after following the recourse recommendations. We repeat the process until the stakeholder’s situation produces a positively labeled point, i.e. a counterfactual.

3.1 An Axiomatically Justified Direction

We axiomatically derive our choice of direction in (1): starting with a set of desirable properties, we identify a direction that uniquely satisfies these properties. More specifically, for a given point of interest $\vec{x} \notin \mathcal{X}_c$, we believe any reasonable recourse direction, denoted by $\vec{d}(\vec{x}, \mathcal{X}_c, f)$ should satisfy the following axioms:

Shift Invariance (SI) Let $\mathcal{X}_c + \vec{b}$ denote the dataset resulting from adding the vector \vec{b} to each point in \mathcal{X} and let $f_{\vec{b}}$ be a shifted model of interest such that $f_{\vec{b}}(\vec{z}) = f(\vec{z} - \vec{b})$ for all \vec{z} . Then, $\vec{d}(\vec{x}, \mathcal{X}_c, f) = \vec{d}(\vec{x} + \vec{b}, \mathcal{X}_c + \vec{b}, f_{\vec{b}})$.

Rotation/Reflection Faithfulness (RRF) Let A be any matrix with $\det(A) \in \{-1, +1\}$ and let $A\mathcal{X}_c$ denote the dataset resulting from replacing every point \vec{x}^j in \mathcal{X}_c with $A\vec{x}^j$. Let f_A denote a rotated model of interest such that $f_A(\vec{z}) = f(A^{-1}\vec{z})$ for all \vec{z} . Then, $A\vec{d}(\vec{x}, \mathcal{X}_c, f) = \vec{d}(A\vec{x}, A\mathcal{X}_c, f_A)$.

Continuity (C) \vec{d} is a continuous function of the dataset \mathcal{X}_c .

Data Manifold Symmetry (DMS) Let f and g be two functions such that $f(\vec{x}^j) = g(\vec{x}^j)$ for all points $\vec{x}^j \in \mathcal{X}$. Then, we must have $\vec{d}(\vec{x}, \mathcal{X}_c, f) = \vec{d}(\vec{x}, \mathcal{X}_c, g)$.

Negative Classification Indifference (NCI) Let $\vec{x}' \in \mathcal{X}_c$ be a datapoint with $f(\vec{x}') = -1$. Then, $\vec{d}(\vec{x}, \mathcal{X}_c, f) = \vec{d}(\vec{x}, \mathcal{X}_c \setminus \{\vec{x}'\}, f)$.

Positive Classification Monotonicity (PCM) Let $\vec{x}' \notin \mathcal{X}_c$ be a point with $f(\vec{x}') = 1$ and $x'_i > x_i$, then $\vec{d}(\vec{x}, \mathcal{X}_c, f) \leq \vec{d}_i(\vec{x}, \mathcal{X}_c \cup \{\vec{x}'\}, f)$. Similarly, if $x'_i < x_i$, then $\vec{d}_i(\vec{x}, \mathcal{X}_c, f) \geq \vec{d}_i(\vec{x}, \mathcal{X}_c \cup \{\vec{x}'\}, f)$.

Our axioms are inspired by the approach of Sliwinski et al. [2019], who identify a family of direction-based explanations, called *Monotone Influence Measures* (MIM), via a similar axiomatic approach. However, unlike the MIM framework, we remove any dependency on points with a negative classification (using the Negative Classification Indifference axiom). Without this change, a naive adaptation of MIM may output directions pointing away from all points in the positive class. Intuitively, having a large number of negative points near positive points may make it impossible to recommend any recourse, as the MIM framework “shies away” from negative point clusters (see a detailed explanation in Appendix A).

The five remaining axioms are fundamental. Shift Invariance and Rotation/Reflection Faithfulness ensure the directions depend on the relative locations of the points rather than their absolute values. The RRF axiom also generalizes the *feature symmetry* axiom, which requires that swapping the coordinates of features i and j not change the value assigned to them; this is commonly used in the characterization of other model explanation frameworks [Datta et al., 2015, 2016, Patel et al., 2021, Lundberg and Lee, 2017, Sliwinski et al., 2019]. In addition, these properties ensure the units in which we measure feature values have no effect on the outcome (e.g. measuring income in dollars rather than cents will not affect the importance placed on income). Continuity ensures that the direction we pick is robust to small changes in the cluster \mathcal{X}_c . Data Manifold Symmetry (DMS) ensures that the direction depends on the model of interest only through points in the dataset. In other words, DMS ensures that the model’s output on points outside the data manifold do not affect the output direction — a desirable property in model explanations [Frye et al., 2021, Lundberg and Lee, 2017, Chen et al., 2020]. Positive Classification Monotonicity (PCM) ensures that the direction will point towards regions with a large number of positively classified points. In other words, if there is a large number of positively classified points with a high value in some feature $i \in N$ (e.g. bank balance), PCM ensures that the output direction will ask the stakeholder to increase their bank balance.

We show that any direction which satisfies the above axioms is uniquely given by (1). Any direction in this family is a weighted combination of the directions from the point of interest to every positively classified point in the dataset. The weight given to every point is a function of their distance $\|\vec{x}' - \vec{x}\|$.

Theorem 3.1. *A recourse direction for a point of interest \vec{x} given a dataset \mathcal{X}_c , a model of interest f and a rotation invariant distance metric $\|\cdot\|$ satisfies SI, RRF, C, DMS, NCI and PCM if and only if it is given by (1).*

The proof is similar to that of Sliwinski et al. [2019, Theorem 4.2] and is relegated to Appendix B.

Reducing the distance that the stakeholder needs to “travel” to reach a positive classification is common objective used in algorithmic recourse [Mothilal et al., 2020a, Karimi et al., 2020a, Mahajan et al., 2019]. This distance can be seen as a measure of the effort required from the stakeholder to change their outcome. We can incorporate this in StEP using the choice of α . Any α function of the form $\alpha(z) = \frac{1}{z^k}$ with $k \geq 2$ ensures that nearby points are assigned a greater weight than far-off points. Different choices of α result in different directions.

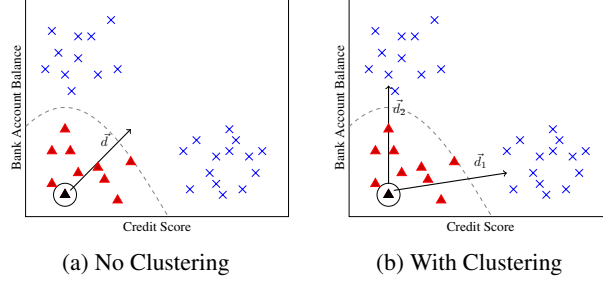


Figure 3: Directly applying the direction formula (1) without clustering to find recourse directions may result in undesirable behavior, e.g. excluding a variety of options and picking an off-manifold direction (Left). Clustering resolves this issue (Right).

3.2 Diverse and On-Manifold Recourse via Clustering

Despite its theoretical soundness, without clustering, StEP has two drawbacks.

Lack of guaranteed diversity: In many cases, changing the α function does not result in a diverse set of directions even when many directions are possible. Consider a slight modification to Example 2.1 (given by Figure 3) where the class of positive points is separated into two clusters. A recourse algorithm could reasonably output a direction towards either cluster as a potential recourse. However, (1) outputs one which is a linear combination of these two clusters. Furthermore, it is easy to see that changing the function α will not significantly change the direction.

Off-manifold directions: Since Equation (1) aggregates directions, it is possible to obtain off-manifold directions (see Figure 3a). This is not ideal since off-manifold regions may have a high prediction error.

Without clustering, Equation (1) aggregates directions obtained for different parts of the dataset, rather than treating different data regions differently. We resolve these issues by clustering the positively classified data points and compute (1) per individual cluster. This ensures that we identify different clusters of points and aggregate each cluster in a theoretically sound manner.

To demonstrate how this modification works, we apply StEP to each instance in Figure 3a and present it in Figure 3b. We can vary the number of generated clusters based on the data and the number of directions we need to generate.

3.3 Privacy-Preserving Direction Selection

One potential concern when using the dataset directly to compute recourse is that StEP could potentially leak sensitive user data (indeed, other model explanation frameworks have been shown to leak private information Milli et al. [2019], Shokri et al. [2021]). With clustering, it may not be possible to offer privacy guarantees since the clustering process itself may not be privacy preserving. However, we can show that the StEP distance computation itself is privacy-preserving (see Dwork and Roth [2014] for a formal exposition to differential privacy). Briefly, an algorithm \mathcal{M} that takes as input a dataset \mathcal{X} and outputs a value $\mathcal{M}(\mathcal{X})$ is said to be (ϵ, δ) -differentially private if for all $S \subseteq \text{range}(\mathcal{M})$, we have:

$$\Pr[\mathcal{M}(\mathcal{X}) \in S] \leq e^\epsilon \Pr[\mathcal{M}(\mathcal{X}') \in S] + \delta$$

where \mathcal{X} and \mathcal{X}' are any two datasets that differ by at most one datapoint. Differential privacy states that the output of \mathcal{M} does not vary much by the removal of any data point. A simple method to prove that a function is differentially private is to upper bound its *sensitivity*, i.e. the change to the function when adding a datapoint. Dwork and Roth [2014] show that adding a finite amount of noise to a bounded sensitivity function guarantees differential privacy. A similar guarantee is offered for Shapley-based [Datta et al., 2016], and gradient-based [Patel et al., 2022] explanations.

StEP (without clustering) can be made differentially private for a specific family of α functions, when the distance metric used is the ℓ_2 norm. More formally, if we assume that $\alpha(z) \leq \frac{C}{z}$ for all $z > 0$, then we can bound the sensitivity of StEP.

Lemma 3.2. *When the distance metric used is the ℓ_2 norm and $\alpha(z) \leq \frac{C}{z}$ for all $z > 0$, the global sensitivity (using the ℓ_2 norm) of the direction given by (1) is upper bounded by C .*

Since the direction has bounded sensitivity, classic results from the differential privacy literature tell us that introducing Gaussian noise makes the direction (ϵ, δ) differentially private.

Theorem 3.3. *When the distance metric used is the ℓ_2 norm and $\alpha(z) \leq \frac{C}{z}$, the directions output by (1) can be made (ϵ, δ) -differentially private by adding Gaussian noise with 0 mean and standard deviation $\sigma \geq \frac{\beta C^2}{\epsilon}$ where $\beta^2 > 2 \log(\frac{1.25}{\delta})$ to all the features.*

This proof of Theorem 3.3 is a direct application of Dwork and Roth [2014, Theorem 3.22] and omitted. When we provide multiple directions to the same user as they progressively improve their datapoint, it is known that the amount (ϵ, δ) of differential privacy guaranteed by the repeated mechanism is equal to the sum of the amount of differential privacy guaranteed by the individual directions. More specifically, if we provide k directions, and each direction is (ϵ, δ) differentially private, then our mechanism is $(k\epsilon, k\delta)$ differentially private [Dwork and Roth, 2014].

4 Empirical Evaluation

We empirically evaluate StEP along with two popular recourse methods for comparison — DiCE [Mothilal et al., 2020a] and FACE [Poyiadzi et al., 2020]. We include full experimental setup details in Appendix F to support reproducibility. Recall that a counterfactual point for \vec{x} is a point \vec{x}_{CF} such that $f(\vec{x}_{CF}) = 1$.

Recourse Baselines Given a negatively classified PoI \vec{x} , DiCE solves an optimization problem that outputs a diverse set of counterfactuals. For each of these counterfactual points \vec{x}_{CF} , $(\vec{x}_{CF} - \vec{x})$ can be interpreted as a direction recommendation for the point \vec{x} . FACE constructs an undirected graph over the set of datapoints and finds a path from the point of interest \vec{x} to a set of positively classified *candidate* points using Dijkstra’s algorithm [Dijkstra, 1959]. Each edge in the path that connects \vec{x} to \vec{x}_{CF} can be thought of as a direction recommendation from \vec{x} to \vec{x}_{CF} .

Given a negatively classified PoI \vec{x} , all three methods (StEP, DiCE, and FACE) result in a sequence of points $(\vec{x}^0, \vec{x}^1, \dots, \vec{x}^\ell)$ where \vec{x}^1 is the PoI after following the first direction recommendation by the recourse method, \vec{x}^2 is the PoI after following the second direction, and so on. We refer to this sequence of points as a *recourse path*. Each of the ℓ directions can be referred to as a “step”.

Datasets and Models We evaluate StEP and the baselines on two real-world datasets: the Credit Card Default [Yeh and Lien, 2009] and the Give Me Some Credit [Credit Fusion, 2011] datasets. Both are financial datasets used to predict whether a user will default on credit card payments or experience financial distress, respectively. For each dataset, we train and validate instances of scikit-learn’s logistic regression and random forest models [Pedregosa et al., 2011] following a 70/15/15 dataset split, where the last 15% is reserved for test-time recourse. For each base model, we specify a confidence threshold of 0.7 at test time, which determines whether a PoI is positively

Method	Success Rate	Proximity	Diversity	Path Length	Number of Steps
StEP	1.00	6.41 ± 0.04	16.11 ± 0.02	6.43 ± 0.04	6.43 ± 0.04
DiCE	1.00	37.84 ± 0.28	117.38 ± 0.81	37.85 ± 0.28	1.00 ± 0.00
FACE	0.16	2.04 ± 0.01	3.74 ± 0.05	2.06 ± 0.02	1.05 ± 0.01

(a) Results on the Credit Card Default dataset using the logistic regression model.

Method	Success Rate	Proximity	Diversity	Path Length	Number of Steps
StEP	0.75	9.01 ± 0.10	100.87 ± 0.03	9.01 ± 0.10	9.01 ± 0.10
DiCE	1.00	82.09 ± 0.29	280.80 ± 0.71	82.09 ± 0.29	1.00 ± 0.00
FACE	0.96	2.36 ± 0.004	3.17 ± 0.01	2.49 ± 0.005	1.26 ± 0.003

(b) Results on the Give Me Some Credit Dataset using the logistic regression model.

Table 1: Comparative analysis results using the logistic regression model. All metrics are averaged and presented along with standard error bounds where applicable. Note that we scale StEP’s directions to have magnitude 1; therefore, the number of steps is always equal to the path length.

classified. Details on model selection and hyperparameter tuning for the base models and recourse methods are described in Appendix F.3.

Properties and Metrics Aligned with the counterfactual and recourse literature, we use the following well-established metrics to evaluate the performance of StEP, DiCE, and FACE on each base model and dataset [Verma et al., 2020]. We also define two appropriate metrics, *path length* and *number of steps* motivated by our direction-based algorithm. In all of the definitions below, we are given a recourse path $(\vec{x}^0, \vec{x}^1, \dots, \vec{x}^\ell)$, where \vec{x}^0 is the PoI \vec{x} . A recourse path is *successful* if $f(\vec{x}^\ell) = 1$, i.e. the recommended path ultimately produced a counterfactual.

Success rate measures the percentage of successful paths generated for a given PoI \vec{x} . This is sometimes referred to as *validity* [Verma et al., 2020].

Proximity is the Euclidean distance between the PoI \vec{x}^0 and the final point \vec{x}^ℓ , i.e. $\|\vec{x}^0 - \vec{x}^\ell\|_2$. Proximity is only computed for successful paths.

Diversity is the sum of the pairwise distances of the terminal points of each of the k recourse paths. Higher diversity translates to a higher degree of variety among counterfactuals. Diversity is only computed for points where all of its recourse paths are successful.

Path length is the sum of Euclidean distances between the steps of a recourse path. A shorter path length requires stakeholders to work less to change their outcome. Formally, the path length is given by $\sum_{i=1}^{\ell} \|\vec{x}^i - \vec{x}^{i-1}\|_2$. Path lengths are only computed for successful paths.

Number of steps corresponds to the number of steps taken in the path, given by $\ell - 1$. When the number of steps is 1 (as is with DiCE), proximity and path length are the same.

4.1 Comparative Analysis of StEP, DiCE, and FACE

We evaluate all combinations of recourse method, base model, and dataset as described in Section 4. All metrics are reported on the original (unscaled) data. For each PoI and each method, we generate $k = 3$ recourse paths and compute metrics and statistics based on the resulting counterfactuals. The comparison of StEP, DiCE, and FACE on the logistic regression model are described in Tables 1a and 1b; due to space constraints, results on the random forest model can be found in Appendix C, along with additional discussion.

Recall that proximity represents the distance between the stakeholder’s original situation (the PoI) and the resulting counterfactual: in general, the higher the proximity, the more time or effort it may take a stakeholder to enact the suggested recourse.

On the Credit Card Default dataset, of the three methods FACE produces counterfactuals with the lowest proximity and path length, which are desirable properties, but at the expense of a very low success rate and diversity score. DiCE obtains a very high diversity and success rate on this task at the cost of obtaining a similarly high proximity/path length. Meanwhile, StEP attains a perfect success rate, along with low proximity and path length and a medium level of diversity. On this task, StEP provides the best trade-offs in produced counterfactuals, particularly when proximity is a priority.

On Give Me Some Credit, FACE obtains a high success rate and low proximity and path length, but produces counterfactuals with very low diversity. As with the previous task, DiCE has an excellent success rate and very high diversity at the cost of very high proximity. While StEP doesn’t produce counterfactuals for every recourse it produces, its successful counterfactuals are of high quality exhibiting the best blend of metric performance with very high diversity and low proximity/path length. Even when a high diversity of counterfactuals is desired, it may be disadvantageous to use DiCE over StEP given the cost in proximity.

FACE is very sensitive to its distance threshold hyperparameter used at graph-generation time. In the case of Credit Card Default, FACE outputs few successful paths, the majority of which in 1 step. This represents a reduction of the algorithm to a simple nearest neighbor search to find a point with distance within the distance threshold for the given model confidence; in other words, the method produces trivial paths in some settings.

Dataset	Noise (β)	Success Rate	Proximity	Diversity	Path Length
Credit Card Default	0	1.00	6.41 ± 0.04	16.11 ± 0.02	6.43 ± 0.04
	0.1	1.00	6.39 ± 0.04	16.06 ± 0.02	6.45 ± 0.05
	0.2	1.00	6.37 ± 0.04	16.00 ± 0.02	6.53 ± 0.05
	0.3	1.00	6.34 ± 0.04	15.96 ± 0.03	6.69 ± 0.05
Give Me Some Credit	0	0.75	9.01 ± 0.10	100.87 ± 0.03	9.01 ± 0.10
	0.1	0.98	10.64 ± 0.07	55.66 ± 0.07	10.69 ± 0.07
	0.2	0.99	9.27 ± 0.05	46.88 ± 0.04	9.44 ± 0.05
	0.3	1.00	8.36 ± 0.05	42.47 ± 0.03	8.71 ± 0.05

Table 2: User-interference experiment results. In this setting, path length and number of steps are always equal, so the latter column is omitted. All metrics are averaged and presented along with standard error bounds where applicable.

Given that StEP produces a recourse path for each cluster it uses, when outliers are present in the dataset used, success rate may be harmed (along with proximity and path length) when one or more of these clusters contains a significant amount of outliers.

4.2 StEP Robustness to User-Interference

In real-world use-cases, user actions may result in “interference” within the recourse model for a many reasons, e.g. inability to carry out the directions along all dimensions. We now relax the assumption that users follow recommended actions exactly by introducing a noise parameter β as a proxy for how much a user deviates or interferes from the prescribed direction.

Noise model: we construct a noise vector where each dimension is independently sampled from the standard normal distribution, then scaled to have magnitude $\beta \times \|\vec{d}\|$, where \vec{d} is the original recourse vector and $\beta \in \mathbb{R}_{\geq 0}^m$. The noise vector is then added to \vec{d} as the next suggested action.

The results presented in Table 2 demonstrate StEP’s robustness to user-interference and other noise. From additional evaluation outlined in Appendix E, the trade-offs observed between diversity and the other metrics in the presence of stochasticity are influenced by the underlying clustering and subspaces of the evaluation data manifold. We elaborate on this explanation in Appendix D accompanied by additional results.

5 Discussion, Limitations and Future Work

We introduce StEP, a novel data-driven framework for direction-based algorithmic recourse that does not depend on the underlying model or knowledge of its underlying causal relations. We show that the directions computed by StEP uniquely satisfy a set of desirable properties, which can be made differentially private under some mild assumptions. We empirically demonstrate StEP’s robustness to user-interference and ability to produce diverse sets of high-quality recourse directions, and show that StEP confers several practical benefits compared to the state-of-the-art.

In Section 3.2, we discuss the limitations of StEP without clustering and highlight the necessity of a clustering-based approach. While having multiple clusters ensures a diverse set of counterfactuals, a fine-grained clustering may result in a decrease to the validity of the resulting explanations. Furthermore, if the dataset contains several outliers, some clusters may contain irrelevant points. We find that standard clustering methods often perform well in practice, though a more thorough analysis of its effects on the StEP framework is left for future work.

The StEP framework (much like DiCE, FACE and Wachter’s method [Wachter et al., 2017]) depends on the way we scale feature values, and more generally on how we measure distances between datapoints. We believe studying different notions of distance and exploring the behavior of StEP using different distances is an important direction for future work. Furthermore, our empirical results reflect performance on datasets of continuous and ordinal features; a meaningful future direction is investigating methods for encoding categorical features in a continuous representation that goes beyond simple one-hot encoding. Capturing non-trivial notions of distance between categorical features is an open problem.

We also believe there are important unanswered questions concerning the group fairness properties of StEP— that is, whether StEP offers similar recourse paths (or even recourse paths of similar length) to similar users from different protected groups. Research on the fairness of explanations is somewhat limited [Balagopalan et al., 2022, Kügelgen et al., 2022]; in particular, we believe that studying the fairness of data-driven algorithmic recourse is an important research direction.

Acknowledgements

The authors would like to thank Neel Patel for being involved in early discussions.

References

- Kjersti Aas, Martin Jullum, and Anders Løland. Explaining individual predictions when features are dependent: More accurate approximations to shapley values. *Artificial Intelligence*, 298, 2021.
- Aparna Balagopalan, Haoran Zhang, Kimia Hamidieh, Thomas Hartvigsen, Frank Rudzicz, and Marzyeh Ghassemi. The road to explainability is paved with bias: Measuring the fairness of explanations. In *Proceedings of the 5th ACM Conference on Fairness, Accountability and Transparency (FAccT)*, pages 1194–1206, 2022.
- Solon Barocas, Andrew D. Selbst, and Manish Raghavan. The hidden assumptions behind counterfactual explanations and principal reasons. In *Proceedings of the 3rd ACM Conference on Fairness, Accountability and Transparency (FAccT)*, pages 80–89, 2020.
- Hugh Chen, Joseph D. Janizek, Scott Lundberg, and Su-In Lee. True to the model or true to the data? In *Proceedings of the 5th Annual Workshop on Human Interpretability in Machine Learning (WHI)*, 2020.
- Will Cukierski Credit Fusion. Give me some credit, 2011. URL <https://kaggle.com/competitions/GiveMeSomeCredit>.
- Amit Datta, Anupam Datta, Ariel D. Procaccia, and Yair Zick. Influence in Classification via Cooperative Game Theory. In *Proceedings of the 24th International Joint Conference on Artificial Intelligence (IJCAI)*, pages 511–517, 2015.
- Anupam Datta, Shayak Sen, and Yair Zick. Algorithmic Transparency via Quantitative Input Influence: Theory and Experiments with Learning Systems. In *Proceedings of the 37th IEEE Conference on Security and Privacy (Oakland)*, pages 598–617, 2016.
- Edsger W Dijkstra. A note on two problems in connexion with graphs. *Numerische mathematik*, 1: 269–271, 1959.
- Cynthia Dwork and Aaron Roth. The algorithmic foundations of differential privacy. *Foundations and Trends in Theoretical Computer Science*, 9(3–4):211–407, 2014.
- Christopher Frye, Damien de Mijolla, Tom Begley, Laurence Cowton, Megan Stanley, and Ilya Feige. Shapley explainability on the data manifold. In *Proceedings of the 9th International Conference on Learning Representations (ICLR)*, 2021.
- Dominik Janzing, Lenon Minorics, and Patrick Blöbaum. Feature relevance quantification in explainable AI: A causal problem. In *Proceedings of the 23rd International Conference on Artificial Intelligence and Statistics (AISTATS)*, pages 2907–2916, 2020.
- Kentaro Kanamori, Takuya Takagi, Ken Kobayashi, and Hiroki Arimura. Dace: Distribution-aware counterfactual explanation by mixed-integer linear optimization. In *Proceedings of the 29th International Joint Conference on Artificial Intelligence (IJCAI)*, pages 2855–2862, 2020.
- Amir-Hossein Karimi, Gilles Barthe, Borja Balle, and Isabel Valera. Model-agnostic counterfactual explanations for sequential decisions. In *Proceedings of the 23rd International Conference on Artificial Intelligence and Statistics (AISTATS)*, pages 895–905, 2020a.

- Amir-Hossein Karimi, Julius von Kügelgen, Bernhard Schölkopf, and Isabel Valera. Algorithmic recourse under imperfect causal knowledge: a probabilistic approach. In *Proceedings of the 33rd Annual Conference on Neural Information Processing Systems (NeurIPS)*, pages 265–277, 2020b.
- Amir-Hossein Karimi, Bernhard Schölkopf, and Isabel Valera. Algorithmic recourse: From counterfactual explanations to interventions. In *Proceedings of the 4th ACM Conference on Fairness, Accountability and Transparency (FAccT)*, pages 353–362, 2021.
- Amir-Hossein Karimi, Gilles Barthe, Bernhard Schölkopf, and Isabel Valera. A survey of algorithmic recourse: Contrastive explanations and consequential recommendations. *ACM Computing Surveys*, 55(5), dec 2022.
- Julius von Kügelgen, Amir-Hossein Karimi, Umang Bhatt, Isabel Valera, Adrian Weller, and Bernhard Schölkopf. On the fairness of causal algorithmic recourse. In *Proceedings of the 36th AAAI Conference on Artificial Intelligence (AAAI)*, pages 9584–9594, 2022.
- Scott M. Lundberg and Su-In Lee. A Unified Approach to Interpreting Model Predictions. In *Proceedings of the 30th Annual Conference on Neural Information Processing Systems (NeurIPS)*, pages 4768–4777, 2017.
- Divyat Mahajan, Chenhao Tan, and Amit Sharma. Preserving causal constraints in counterfactual explanations for machine learning classifiers. *ArXiv*, abs/1912.03277, 2019.
- Smitha Milli, Ludwig Schmidt, Anca D. Dragan, and Moritz Hardt. Model Reconstruction from Model Explanations. In *Proceedings of the 1st ACM Conference on Fairness, Accountability and Transparency (FAT*)*, pages 1–9, 2019.
- Ramaravind K. Mothilal, Amit Sharma, and Chenhao Tan. Explaining machine learning classifiers through diverse counterfactual explanations. In *Proceedings of the 3rd ACM Conference on Fairness, Accountability and Transparency (FAccT)*, page 607–617, 2020a.
- Ramaravind K. Mothilal, Amit Sharma, and Chenhao Tan. Explaining machine learning classifiers through diverse counterfactual examples. In *Proceedings of the 3rd ACM Conference on Fairness, Accountability and Transparency (FAccT)*, 2020b.
- Neel Patel, Martin Strobel, and Yair Zick. High dimensional model explanations: an axiomatic approach. In *Proceedings of the 4th ACM Conference on Fairness, Accountability and Transparency (FAccT)*, pages 401–411, 2021.
- Neel Patel, Reza Shokri, and Yair Zick. Model explanations with differential privacy. In *Proceedings of the 2022 ACM Conference on Fairness, Accountability and Transparency (FAccT)*, page 1895–1904, 2022.
- F. Pedregosa, G. Varoquaux, A. Gramfort, V. Michel, B. Thirion, O. Grisel, M. Blondel, P. Prettenhofer, R. Weiss, V. Dubourg, J. Vanderplas, A. Passos, D. Cournapeau, M. Brucher, M. Perrot, and E. Duchesnay. Scikit-learn: Machine learning in Python. *Journal of Machine Learning Research*, 12:2825–2830, 2011.
- Rafael Poyiadzi, Kacper Sokol, Raul Santos-Rodriguez, Tijl De Bie, and Peter Flach. FACE: Feasible and actionable counterfactual explanations. In *Proceedings of the 3rd AAAI/ACM Conference on Artificial Intelligence, Ethics and Society (AIES)*, page 344–350, 2020.
- Marco T. Ribeiro, Sameer Singh, and Carlos Guestrin. Why Should I Trust You?: Explaining the Predictions of Any Classifier. In *Proceedings of the 22nd International Conference on Knowledge Discovery and Data Mining (KDD)*, pages 1135–1144, 2016.
- Reza Shokri, Martin Strobel, and Yair Zick. On the privacy risks of model explanations. In *Proceedings of the 4th AAAI/ACM Conference on Artificial Intelligence, Ethics and Society (AIES)*, 2021.
- Karen Simonyan, Andrea Vedaldi, and Andrew Zisserman. Deep inside convolutional networks: Visualising image classification models and saliency maps. *arXiv preprint arXiv:1312.6034*, 2013.

- Dylan Slack, Sophie Hilgard, Emily Jia, Sameer Singh, and Himabindu Lakkaraju. Fooling LIME and SHAP: Adversarial attacks on post hoc explanation methods. In *Proceedings of the 3rd AAAI/ACM Conference on Artificial Intelligence, Ethics and Society (AIES)*, pages 180–186, 2020.
- Dylan Slack, Anna Hilgard, Himabindu Lakkaraju, and Sameer Singh. Counterfactual explanations can be manipulated. *Proceedings of the 34th Annual Conference on Neural Information Processing Systems (NeurIPS)*, pages 62–75, 2021.
- Jakub Sliwinski, Martin Strobel, and Yair Zick. A Characterization of Monotone Influence Measures for Data Classification. In *Proceedings of the 33rd AAAI Conference on Artificial Intelligence (AAAI)*, pages 718–725, 2019.
- Berk Ustun, Alexander Spangher, and Yang Liu. Actionable recourse in linear classification. In *Proceedings of the 2nd ACM Conference on Fairness, Accountability and Transparency (FAccT)*, page 10–19, 2019.
- Sahil Verma, John Dickerson, and Keegan Hines. Counterfactual explanations for machine learning: A review, 2020.
- Sandra Wachter, Brent Mittelstadt, and Luciano Floridi. Why a right to explanation of automated decision-making does not exist in the general data protection regulation. *International Data Privacy Law*, 7(2):76–99, 2017.
- Sandra Wachter, Brent Mittelstadt, and Chris Russell. Counterfactual explanations without opening the black box: automated decisions and the GDPR. *Harvard Journal of Law & Technology*, 31, 2018.
- I-Cheng Yeh and Chehui Lien. The comparisons of data mining techniques for the predictive accuracy of probability of default of credit card clients. *Expert Systems with Applications*, 36(2, Part 1):2473–2480, 2009.

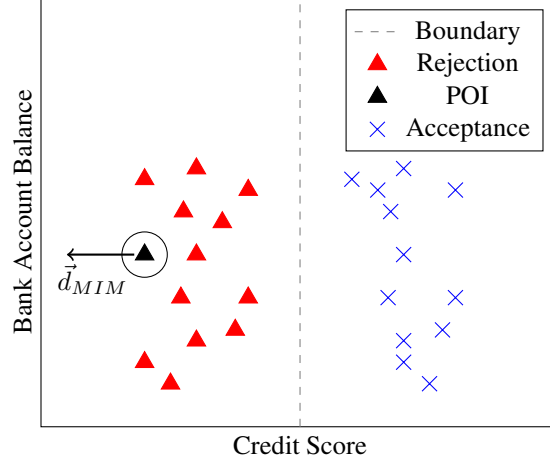


Figure 4: An example where the MIM direction points away from all the positively classified points.

A Issue with the Naive Adaptation of MIM

MIM (proposed by Sliwinski et al. [2019]) is a data driven approach to explain the outcome of point \vec{x} . Intuitively, it is a direction that moves towards points of the same outcome and moves away from points of the opposite outcome. It is given by:

$$\vec{d}(\vec{x}, \mathcal{X}, f) = \sum_{\vec{x}' \in \mathcal{X}} (\vec{x}' - \vec{x}) \alpha(\|\vec{x}' - \vec{x}\|) \mathbb{1}(f(\vec{x}') = f(\vec{x}))$$

where α is a non-negative valued function and $\mathbb{1}(\cdot)$ takes the value 1 if the input condition is true and 0 otherwise. We can naively adapt MIM for recourse by flipping the direction, moving towards positively classified points and away from negatively classified points. This would give us the direction:

$$\vec{d}(\vec{x}, \mathcal{X}, f) = \sum_{\vec{x}' \in \mathcal{X}} (\vec{x}' - \vec{x}) \alpha(\|\vec{x}' - \vec{x}\|) \mathbb{1}(f(\vec{x}') \neq f(\vec{x}))$$

This direction, unfortunately, can lead to bad recourse recommendations. To see why, consider Example 2.1 with a different dataset and point of interest (given in Figure 4). When nearby points are given a higher weight than far away points, the direction output by MIM could be poor, pointing away from all the positively classified points. This is because when nearby points are given a higher weight than far away points, the push away from negatively classified points can be stronger than the pull towards positively classified points. This is indeed what happens in Figure 4.

B Missing Proofs from Section 3

Theorem 3.1. *A recourse direction for a point of interest \vec{x} given a dataset \mathcal{X}_c , a model of interest f and a rotation invariant distance metric $\|\cdot\|$ satisfies SI, RRF, C, DMS, NCI and PCM if and only if it is given by (1).*

Proof. For readability, we replace \mathcal{X}_c with \mathcal{X} . It is easy to see that (1) satisfies all five axioms so we only show uniqueness.

We assume without loss of generality that \mathcal{X} contains no negatively classified points. If \mathcal{X} does contain any negatively classified points, we can simply remove them without changing the recourse direction because of Negative Classification Indifference (NCI). Therefore, our goal is to show that any direction which satisfies (SI), (RRF), (C), (DMS), (NCI) and (PCM) is of the form

$$\vec{d}(\vec{x}, \mathcal{X}, f) = \sum_{\vec{x}' \in \mathcal{X}} \alpha(\|\vec{x}' - \vec{x}\|) (\vec{x}' - \vec{x})$$

We start off with a useful lemma.

Lemma B.1. *If any direction \vec{d} satisfies Rotation and Reflection Faithfulness (RRF) and Positive Classification Monotonicity (PCM), then for any dataset \mathcal{X} , any datapoint \vec{x} , any model of interest f and any positively classified point $\vec{y} \neq \vec{x}$, there exists some $a \geq 0$ such that*

$$\vec{d}(\vec{x}, \mathcal{X} \cup \{\vec{y}\}, f) - \vec{d}(\vec{x}, \mathcal{X}, f) = a(\vec{y} - \vec{x})$$

Proof. Suppose for contradiction that there is some $\vec{x}, \mathcal{X}, \vec{y}$ and f such that

$$\forall a \geq 0 : \vec{d}(\vec{x}, \mathcal{X} \cup \{\vec{y}\}, f) - \vec{d}(\vec{x}, \mathcal{X}, f) \neq a(\vec{y} - \vec{x})$$

Let $\vec{l} = \vec{d}(\vec{x}, \mathcal{X} \cup \{\vec{y}\}, f) - \vec{d}(\vec{x}, \mathcal{X}, f)$. Let A be a rotation matrix such that $(A\vec{l})_1 < 0$ and $[A(\vec{y} - \vec{x})]_1 > 0$; such a matrix exists since the two vectors are either linearly independent or $\vec{l} = -b(\vec{y} - \vec{x})$ where $b \in \mathbb{R}^+$. Since \vec{d} satisfies Rotation and Reflection Faithfulness (RRF), we have from $(A\vec{l})_1 < 0$

$$\vec{d}_1(A\vec{x}, A\mathcal{X} \cup \{A\vec{y}\}, f_A) - \vec{d}_1(A\vec{x}, A\mathcal{X}, f_A) < 0$$

This contradicts the Positive Classification Monotonicity (PCM) property since $(A\vec{y})_1 > (A\vec{x})_1$ and $f_A(A\vec{y}) = f(\vec{y}) = 1$. \square

Consider a direction \vec{d} that satisfies the 6 desired axioms. We go ahead and show uniqueness via induction on $|\mathcal{X}|$. Let $k = 0, \mathcal{X} = \{\}$. By Shift Invariance (SI), $\vec{d}(\vec{x}, \{\}, f) = \vec{d}(\vec{0}, \{\}, f_{-\vec{x}})$. The vector $\vec{0}$ and an empty \mathcal{X} are invariant under rotation. Therefore, since \vec{d} satisfies Rotation and Reflection Faithfulness (RRF) and Data Manifold Symmetry (DMS), we must have $\vec{d}(\vec{0}, \{\}, f_{-\vec{x}}) = \vec{0}$, the only vector invariant under rotation.

Let $k = 1, \mathcal{X} = \{\vec{y}\}$ where $\vec{y} \neq \vec{x}$. Note that any pair of (\vec{x}, \vec{y}) can be translated by shift and rotation to any other pair (\vec{x}', \vec{y}') with the same distance ($\|\vec{y} - \vec{x}\|$) between them. This is because the distance metric ($\|\cdot\|$) is rotation invariant and any distance metric is shift invariant when computing the distance between two points; the shifts cancel each other out. Note that after rotation by some matrix A , we have $f_A(A\vec{y}) = f(\vec{y})$ and similarly, after shift by some vector \vec{b} , we have $f_{\vec{b}}(\vec{y} + \vec{b}) = f(\vec{y})$. Therefore, the label of the point y does not change after applying Shift Invariance (SI) or Rotation and Reflection Faithfulness (RRF). Therefore, by (SI), (RRF) and Lemma B.1, we have

$$\vec{d}(\vec{x}, \mathcal{X}, f) = \alpha(\|\vec{y} - \vec{x}\|)(\vec{y} - \vec{x})$$

where α is a non-negative valued function.

Suppose the hypothesis holds when $|\mathcal{X}| \leq k$. Consider a dataset \mathcal{Y} of size $k + 1$. This means \mathcal{Y} contains at least two distinct points $\vec{y}, \vec{z} \neq \vec{x}$. We prove our hypothesis for the case where \vec{y} and \vec{z} are linearly independent. The case where they are linearly dependent follows from Continuity (C): we can perturb the vectors slightly to make them linearly independent. By Lemma B.1, we have

$$\begin{aligned} \vec{d}(\vec{x}, \mathcal{Y}, f) &\in A = \{\vec{d}(\vec{x}, \mathcal{Y} \setminus \{\vec{y}\}, f) + a(\vec{y} - \vec{x})\} \\ \text{and } \vec{d}(\vec{x}, \mathcal{Y}, f) &\in B = \{\vec{d}(\vec{x}, \mathcal{Y} \setminus \{\vec{z}\}, f) + a(\vec{z} - \vec{x})\} \end{aligned} \quad (2)$$

By the inductive hypothesis, we have

$$\begin{aligned} \vec{d}(\vec{x}, \mathcal{Y} \setminus \{\vec{y}\}, f) &= \vec{d}(\vec{x}, \mathcal{Y} \setminus \{\vec{y}, \vec{z}\}, f) + \alpha(\|\vec{z} - \vec{x}\|)(\vec{z} - \vec{x}) \\ \text{and } \vec{d}(\vec{x}, \mathcal{Y} \setminus \{\vec{z}\}, f) &= \vec{d}(\vec{x}, \mathcal{Y} \setminus \{\vec{y}, \vec{z}\}, f) + \alpha(\|\vec{y} - \vec{x}\|)(\vec{y} - \vec{x}) \end{aligned}$$

We can use this and the fact that $\vec{y} - \vec{x}$ and $\vec{z} - \vec{x}$ are linearly independent to combine the two sets in (2) to get

$$\begin{aligned} \vec{d}(\vec{x}, \mathcal{Y}, f) &= A \cap B \\ &= \vec{d}(\vec{x}, \mathcal{Y} \setminus \{\vec{y}, \vec{z}\}, f) + \alpha(\|\vec{y} - \vec{x}\|)(\vec{y} - \vec{x}) + \alpha(\|\vec{z} - \vec{x}\|)(\vec{z} - \vec{x}) \end{aligned}$$

This completes the induction. \square

Lemma 3.2. *When the distance metric used is the ℓ_2 norm and $\alpha(z) \leq \frac{C}{z}$ for all $z > 0$, the global sensitivity (using the ℓ_2 norm) of the direction given by (1) is upper bounded by C .*

Proof. Let the direction output of (1) (in the absence of clustering) for a particular dataset \mathcal{X} , a model of interest f and a point of interest \vec{x} be $\vec{d}(\vec{x}, \mathcal{X}, f)$.

The global sensitivity of (1) using the l_2 norm is given by

$$\Delta_2 \vec{d} = \max_{\vec{x}, \mathcal{X}, \mathcal{X}'} \|\vec{d}(\vec{x}, \mathcal{X}, f) - \vec{d}(\vec{x}, \mathcal{X}', f)\|_2 \quad (3)$$

where \mathcal{X}' is \mathcal{X} with one additional (or one less) datapoint [Dwork and Roth, 2014]. We can assume without loss of generality that \mathcal{X}' contains one additional positively classified datapoint \vec{x}' . If the point is not positively classified, then none of the directions change and the sensitivity is 0. The global sensitivity defined in (3) reduces to

$$\begin{aligned} \Delta_2 \vec{d} &= \max_{\vec{x}, \vec{x}'} \|(\vec{x}' - \vec{x})\alpha(\|\vec{x}' - \vec{x}\|_2)\mathbb{I}(f(\vec{x}') = 1)\|_2 \\ &\leq \max_{\vec{x}, \vec{x}'} \left\| (\vec{x}' - \vec{x}) \frac{C}{\|\vec{x}' - \vec{x}\|_2} \right\|_2 && \text{(from our assumptions on } \alpha \text{ and } f(\vec{x}')) \\ &\leq \max_{\vec{x}, \vec{x}'} \frac{1}{\|\vec{x}' - \vec{x}\|_2} \|C(\vec{x}' - \vec{x})\|_2 \\ &= C \end{aligned}$$

In the first inequality, we assume $\|\vec{x} - \vec{x}'\|_2 > 0$ so we can apply $\alpha(\|\vec{x} - \vec{x}'\|_2) \leq \frac{C}{\|\vec{x} - \vec{x}'\|_2}$. If $\|\vec{x} - \vec{x}'\|_2 = 0$, then by definition we must have $\vec{x} = \vec{x}'$ which implies $\Delta_2 \vec{d} = 0$ and the lemma trivially holds. \square

C Additional Comparison of StEP, DiCE, and FACE

We compare StEP with two popular methods, DiCE and FACE by generating $k = 3$ recourse instructions for each negatively classified datapoint in the test set for each dataset.

With StEP, we first partition the positively labeled training data into 3 clusters, and then for each PoI in the test set, we produce a direction for each of the 3 clusters. In these comparative experiments, we use sci-kit learn’s default k-means implementation without any tuning, and we assume the the stakeholder follows the provided direction exactly.

C.1 Additional Comparative Analysis Results

Table 3 presents results with the random forest model on both the Credit Card Default and Give Me Some Credit datasets. We also measure two new metrics defined below.

Partial success rate (or Partial Success) measures the fraction of points for which at least one of the k recourse paths is successful.

Diversity with Partial Success (Diversity wPS) is the sum of the pairwise distances of the terminal points of each of the *successful* recourse paths for a given point of interest. Diversity wPS is only computed on points with at least one successful recourse path.

The results for these new metrics are presented in Table 4. Surprisingly, StEP is the *only* method with with a partial success rate of 1 in all our experiments. For both DiCE and FACE, there are instances where the method fails to output a successful recourse path despite being allowed three attempts. StEP’s partial success also corroborates our results indicating that the underlying cluster quality influences StEP’s performance, and that StEP remains robust in light of sub-optimal clustering.

C.2 Discussion of DiCE

Since DiCE is not a direction-based method, we generate k counterfactual points and interpret the difference between the original PoI \vec{x} and counterfactual \vec{x}_{CF} as a proxy for the path to take.

In our experiments, DiCE almost always generates a valid counterfactual explanation but this counterfactual is usually much farther from the PoI than StEP on average, which requires the user to make very large changes at each step of recourse. Furthermore, sometimes the counterfactual can be away from the data manifold and infeasible.

Method	Success Rate	Proximity	Diversity	Path Length	Number of Steps
StEP	0.86	3.28 ± 0.06	8.05 ± 0.10	5.27 ± 0.19	5.27 ± 0.19
DiCE	1.00	27.96 ± 0.47	98.80 ± 1.01	27.96 ± 0.47	1.00 ± 0.00
FACE	0.86	1.91 ± 0.00	5.57 ± 0.05	0.89 ± 0.00	1.00 ± 0.00

(a) Results on the Credit Card Default dataset using the random forest model.

Method	Success Rate	Proximity	Diversity	Path Length	Number of Steps
StEP	0.97	16.74 ± 0.49	93.29 ± 0.30	16.91 ± 0.50	16.91 ± 0.50
DiCE	0.85	65.32 ± 1.26	243.99 ± 3.04	65.32 ± 1.26	1.00 ± 0.00
FACE	1.00	1.99 ± 0.00	5.32 ± 0.04	1.99 ± 0.00	1.00 ± 0.00

(b) Results on the Give Me Some Credit Dataset using the random forest model.

Table 3: Comparative analysis results using the random forest model. All metrics are averaged and presented along with standard error bounds where applicable. Note that we scale StEP’s directions to have magnitude 1; therefore, the number of steps is always equal to the path length.

Method	Partial Success	Diversity wPS
StEP	1.00	16.11 ± 0.02
DiCE	1.00	117.38 ± 0.81
FACE	0.17	3.66 ± 0.05

(a) Results on the Credit Card Default dataset using the logistic regression model.

Method	Partial Success	Diversity wPS
StEP	1.00	37.81 ± 0.32
DiCE	1.00	280.80 ± 0.71
FACE	0.96	3.17 ± 0.01

(b) Results on the Give Me Some Credit Dataset using the logistic regression model.

Method	Partial Success	Diversity wPS
StEP	1.00	6.36 ± 0.10
DiCE	1.00	98.80 ± 1.01
FACE	0.91	5.36 ± 0.06

(c) Results on the Credit Card Default dataset using the random forest model.

Method	Partial Success	Diversity wPS
StEP	1.00	89.40 ± 0.45
DiCE	0.99	207.75 ± 0.45
FACE	1.00	5.32 ± 0.04

(d) Results on the Give Me Some Credit Dataset using the random forest model.

Table 4: Comparative analysis results for the metrics partial success rate and diversity wPS. All metrics are averaged and presented along with standard error bounds where applicable.

Specifically, we found that in one instance in the Credit Card Default task, DiCE output a counterfactual point with a bill amount of -14905 ; in other words, expecting that the stakeholder pay a negative sum on their credit card, which is infeasible.

C.3 Discussion of FACE

FACE is a direction-based recourse method which finds the shortest path from each PoI \vec{x} to k positively classified candidate points that exist within the graph (i.e. counterfactuals). The existence of edges between points in a graph are determined using a *distance threshold* parameter. If two points have a distance less than the distance threshold, an edge is generated; otherwise, no edge spans the two points. Intuitively, the distance threshold determines the size of the step users are required to take when following FACE’s recourse.

Finding an appropriate distance threshold for FACE is a challenging and highly task-dependent requirement. If the distance threshold is too small, the graph becomes sparse and typically produces few to no successful recourse paths. On the other hand, if the distance threshold is very large, the graph becomes dense and recourse generates trivial paths between PoIs and candidate points consisting of a single edge. In this case, FACE produces a brittle recourse.

One possible option for the distance threshold is to set it equal to the step-size of StEP (equal to 1) to ensure a fair comparison of the two methods, which results in very few successful paths being

generated (in some tasks, with a success rate as low as 0). When increasing the distance threshold to 2, FACE begins non-trivial paths across our tasks. All the results generated in this paper are using the distance threshold 2.

Dataset	Noise (β)	Success Rate	Proximity	Diversity	Path Length
Credit Card Default	0	1.00	6.41 ± 0.04	16.11 ± 0.02	6.43 ± 0.04
	0.1	1.00	6.39 ± 0.04	16.06 ± 0.02	6.45 ± 0.05
	0.2	1.00	6.37 ± 0.04	16.00 ± 0.02	6.53 ± 0.05
	0.3	1.00	6.34 ± 0.04	15.96 ± 0.03	6.69 ± 0.05
	0.5	1.00	6.27 ± 0.05	15.89 ± 0.03	7.16 ± 0.05
	0.75	1.00	6.13 ± 0.05	15.83 ± 0.03	7.99 ± 0.06
	1.0	1.00	6.04 ± 0.05	15.56 ± 0.04	9.05 ± 0.07
Give Me Some Credit	0	0.75	9.01 ± 0.10	100.87 ± 0.03	9.01 ± 0.10
	0.1	0.98	10.64 ± 0.07	55.66 ± 0.07	10.69 ± 0.07
	0.2	0.99	9.27 ± 0.05	46.88 ± 0.04	9.44 ± 0.05
	0.3	1.00	8.36 ± 0.05	42.47 ± 0.03	8.71 ± 0.05
	0.5	1.00	6.68 ± 0.04	34.14 ± 0.06	7.42 ± 0.04
	0.75	1.00	4.94 ± 0.03	24.65 ± 0.07	6.12 ± 0.04
	1.0	1.00	4.43 ± 0.03	21.98 ± 0.06	6.29 ± 0.04

Table 5: Complete user-interference experiment results with the logistic regression model. In this setting, path length and number of steps are always equal, so the latter column is omitted. All metrics are averaged and presented along with standard error bounds where applicable.

Dataset	Noise (β)	Success Rate	Proximity	Diversity	Path Length
Credit Card Default	0	0.86	3.28 ± 0.06	8.05 ± 0.10	5.27 ± 0.19
	0.1	0.93	3.39 ± 0.06	8.60 ± 0.08	6.69 ± 0.24
	0.2	0.98	3.38 ± 0.06	8.81 ± 0.08	7.00 ± 0.23
	0.3	1.00	3.43 ± 0.06	8.93 ± 0.08	5.66 ± 0.14
	0.5	1.00	3.38 ± 0.05	8.84 ± 0.08	5.48 ± 0.13
	0.75	1.00	3.33 ± 0.05	9.45 ± 0.09	5.36 ± 0.11
	1.0	1.00	3.14 ± 0.05	9.11 ± 0.08	5.95 ± 0.14
Give Me Some Credit	0	1.00	16.08 ± 0.46	91.39 ± 0.39	16.26 ± 0.47
	0.1	1.00	1.07 ± 0.01	4.40 ± 0.03	1.07 ± 0.01
	0.2	1.00	1.06 ± 0.01	4.35 ± 0.02	1.06 ± 0.01
	0.3	1.00	1.05 ± 0.01	4.33 ± 0.02	1.05 ± 0.01
	0.5	1.00	1.04 ± 0.00	4.30 ± 0.02	1.04 ± 0.01
	0.75	1.00	1.05 ± 0.01	4.42 ± 0.02	1.07 ± 0.01
	1.0	1.00	1.04 ± 0.00	4.40 ± 0.02	1.07 ± 0.01

Table 6: Complete user-interference experiment results with the random forest model. In this setting, path length and number of steps are always equal, so the latter column is omitted. All metrics are averaged and presented along with standard error bounds where applicable.

D Additional StEP User-Interference Results

The noise β we introduce offers insights into StEP’s behavior. Interestingly, introducing noise actually results in *better* performance on the Give Me Some Credit Dataset (Table 2). The reason for this behavior appears to be the clusters we produce. StEP clusters the *positively* labeled evaluation data which introduces additional hyperparameters: the number of clusters, k , and the clustering method. We cluster the evaluation data in full *without removing any outliers*. In particular, one cluster in the Give Me Some Credit dataset contained several outliers.

When generating recourse for a PoI \vec{x} , StEP produces a direction towards the centers of each of the k clusters. Any outliers in the evaluation data can cause dramatic shifts in the directions, due to the sparse topology of the outlier clusters.

Dataset	Noise (β)	Logistic Regression		Random Forest	
		Partial Success	Diversity wPS	Partial Success	Diversity wPS
Credit Card Default	0	1.00	16.11 \pm 0.02	1.00	6.36 \pm 0.10
	0.1	1.00	16.06 \pm 0.02	1.00	7.73 \pm 0.09
	0.2	1.00	16.00 \pm 0.02	1.00	8.57 \pm 0.08
	0.3	1.00	15.96 \pm 0.02	1.00	8.93 \pm 0.08
	0.5	1.00	15.89 \pm 0.03	1.00	8.84 \pm 0.08
	0.75	1.00	15.82 \pm 0.03	1.00	9.45 \pm 0.09
	1.0	1.00	15.56 \pm 0.04	1.00	9.11 \pm 0.08
Give Me Some Credit	0	1.00	37.81 \pm 0.32	1.00	91.30 \pm 0.39
	0.1	1.00	53.73 \pm 0.09	1.00	4.40 \pm 0.03
	0.2	1.00	46.62 \pm 0.04	1.00	4.35 \pm 0.02
	0.3	1.00	42.34 \pm 0.03	1.00	4.33 \pm 0.02
	0.5	1.00	34.13 \pm 0.06	1.00	4.30 \pm 0.02
	0.75	1.00	24.65 \pm 0.07	1.00	4.42 \pm 0.02
	1.0	1.00	21.98 \pm 0.07	1.00	4.40 \pm 0.02

Table 7: Additional user-interference experiment results. In this setting, path length and number of steps are always equal, so the latter column is omitted. All metrics are averaged and presented along with standard error bounds where applicable.

The Give Me Some Credit dataset exhibits significant variance between the mean path length across the clusters. Beyond removing outliers from the dataset, we suggest the following to correct for the variance influenced by the presence of outliers: (a) increase the number of clusters used and ignore the paths computed for a cluster which has an average path length of ≥ 2 standard deviations higher than the mean path length between the other clusters; (b) increasing the number of clusters may help disperse the cluster assignments of outliers, and the more clusters StEP uses results in more paths produced, which can help support generating a greater number of viable suggested recourse options for a given stakeholder.

In Tables 5 and 6, we present results for a wide range of choices of the noise parameter β . We also present results on the partial success and diversity wPS metrics (defined in Section C.1) in Table 7.

E StEP Clustering

In Table 8, we present results when varying the number of clusters initialized for StEP. For each of the k clusters, StEP produces recourse. For $k \in \{3, 4, 5\}$ using the logistic regression model on each dataset, success rate is high and roughly stable across all values, while diversity consistently increases as k increases. We expect diversity to increase as a function of k because this metric represents the sum of pairwise distances between the PoI and each counterfactual. This represents a design choice for practitioners using StEP, particularly when diversity is an important property.

F Experimental Details for Reproducibility

F.1 Baseline Recourse Methods

We compare StEP to DiCE [Mothilal et al., 2020a] and FACE [Poyiadzi et al., 2020]. DiCE outputs a diverse set of points while FACE outputs a set of paths that terminate at a positively classified point.

Given a point \vec{x} such that $f(\vec{x}) = -1$, DiCE uses determinantal point processes and solves the following optimization problem to output a diverse set of m counterfactual explanations $\{\vec{c}_1, \vec{c}_2, \dots, \vec{c}_m\}$:

$$\arg \min_{\vec{c}_1, \vec{c}_2, \dots, \vec{c}_m} \frac{1}{m} \sum_{i=1}^m \text{loss}(f(\vec{c}_i), 1) + \frac{\lambda_1}{m} \sum_{i=1}^m \text{dist}(\vec{c}_i, \vec{x}) - \lambda_2 \text{dpp_diversity}(\vec{c}_1, \vec{c}_2, \dots, \vec{c}_m)$$

Dataset	Num. Clusters	Success Rate	Proximity	Diversity	Path Length
Credit Card Default	3	1.00	6.41 ± 0.04	16.11 ± 0.02	6.43 ± 0.04
	4	1.00	7.01 ± 0.04	45.93 ± 0.15	7.04 ± 0.04
	5	1.00	6.83 ± 0.04	68.95 ± 0.20	6.85 ± 0.04
Give Me Some Credit	3	0.97	16.74 ± 0.49	93.29 ± 0.30	16.91 ± 0.50
	4	0.93	16.49 ± 0.40	178.35 ± 1.05	16.63 ± 0.41
	5	0.94	13.56 ± 0.34	245.03 ± 1.31	13.67 ± 0.34

(a) Results with the logistic regression model.

Dataset	Num. Clusters	Success Rate	Proximity	Diversity	Path Length
Credit Card Default	3	0.86	3.28 ± 0.06	8.05 ± 0.10	5.27 ± 0.19
	4	0.88	3.41 ± 0.06	15.54 ± 0.19	4.70 ± 0.14
	5	0.89	3.31 ± 0.05	25.72 ± 0.33	4.10 ± 0.10
Give Me Some Credit	3	0.75	9.01 ± 0.10	100.87 ± 0.03	9.01 ± 0.10
	4	0.80	16.67 ± 0.10	214.13 ± 0.05	16.67 ± 0.10
	5	0.84	13.51 ± 0.08	296.82 ± 0.07	13.51 ± 0.08

(b) Results with the random forest model.

Table 8: StEP clustering evaluation. In this setting, path length and number of steps are always equal, so the latter column is omitted. All metrics are averaged and presented along with standard error bounds.

Each of the output points \vec{c}_j can be seen as a recommendation for the direction $\vec{c}_j - \vec{x}$. Due to the structure of the optimization problem, none of these output points are guaranteed to be positively classified. We run DiCE with the default hyperparameter settings.

To obtain a set of m paths from DiCE, we first obtain m directions from DiCE and move the point along each direction to get a set of m points which correspond to the DiCE outputs $\{\vec{c}_1, \dots, \vec{c}_m\}$. If any of these points (say \vec{c}_i) fail to achieve a positive classification, we run DiCE again generating m counterfactual explanations starting at \vec{c}_i and pick one random counterfactual explanation. This procedure gives us a sequence of m diverse paths from any point of interest \vec{x} .

FACE constructs an undirected graph over the set of data points and finds a path from the point of interest to a set of positively classified *candidate* points using Dijkstra’s algorithm [Dijkstra, 1959].

F.2 Datasets Details

Credit Card Default: we produce random train, validation, and test sets from the 30,000 instances using a 0/15/15 split, resulting in sets with approximately 21k/4.5k/4.5k datapoints respectively. The label distribution across splits is balanced such that each split has roughly half positively and negatively labeled points. This dataset contains 24 features.

Give Me Some Credit: we produce randomly assigned train, validation, and test splits from the instances in the same manner as with Credit Card Default, maintaining balanced label distribution across the splits. Give Me Some Credit consists of 10 features.

F.3 Base Model Details

Each method relies on a base machine learning model; in our experiments, we use sci-kit learn’s implementation of logistic regression and random forest under the assumption that downstream practitioners of the StEP algorithm would prefer simpler and more explainable models. We use simple holdout set validation to determine the hyperparameters used, outlined in F.5.

F.4 StEP Parameters Discussion

Choosing a Distance Metric: We use the simple rotation invariant ℓ_2 -norm as our distance metric. To ensure the distance function is not biased towards any feature, we normalize continuous feature values with respect to their mean and standard deviation (Mothilal et al. [2020b] follow a similar

methodology). More formally, for a continuous feature i , we transform its value as follows:

$$x_i^j := \frac{1}{\sigma_i}(x_i^j - \mu_i)$$

where μ_i is the mean value of the feature and σ_i is the standard deviation.

Choosing the α function We propose two different α functions — the *volcano* function¹ and the *sloped* function. The volcano function weighs nearby points higher than faraway points, but all points closer than a specific threshold are weighed equally (a similar function is used by Patel et al. [2022]). We denote this function by α_v and define it as follows:

$$\alpha_v(z; d, \gamma) = \begin{cases} \frac{1}{z^d} & z > \gamma \\ \frac{1}{\gamma^d} & z \leq \gamma \end{cases} \tag{4}$$

The sloped function is shaped like a normal distribution curve with a 0 mean. We denote this function by α_s and define it as follows

$$\alpha_s(z; w) = \exp\left(-\frac{1}{2}\left(\frac{z}{w}\right)^2\right)$$

Both of these functions are continuous and upper bounded. If we divide the output of these functions by z (the input to the functions), the output will satisfy the conditions of Theorem 3.3, i.e. the MRM framework can be made differentially private with a slightly modified version of these α functions.

In our experiments, we use the volcano function α_v with $d = 2$ and $\gamma = 0.5$.

F.5 Other Hyperparameter Selection

We perform a basic grid search across base models, recourse methods, and datasets using sci-kit learn’s GridSearchCV function. To determine appropriate hyperparameters to use across the base ML models and recourse methods, we roughly optimize for a reasonably high success rate and to minimize average overall path length.

For each base ML model, we sweep over a confidence cutoff between $\{0.6, 0.7, 0.8, 0.9\}$ and evaluate the performance of each recourse method. We find that 0.7 provides reasonable results across datasets, base models, and recourse methods while remaining a reasonable value a practitioner may use. We vary $k \in \{1, 2, 3, 4, 5\}$, the number of paths to produce for each PoI (and for StEP, the number of clusters to produce), and fix $k = 3$ for our comparative analysis and user-interference experiments.

For StEP, we consider step sizes in $\{0.5, 1, 2, 4\}$ and fix a value of 1 across all experiments. FACE has two main hyperparameters: graph type in $\{k\text{-NN}, \epsilon, \text{KDE}\}$ and distance threshold (a float). In C.3, we provide substantial discussion on the distance threshold parameter. For all our experiments using FACE, we used the ϵ graph following a suggestion from the authors of the method. For all recourse methods, we allowed a maximum of 50 iterations to produce a counterfactual.

F.6 Computational Resources Used

We used a distributed cluster for our empirical evaluation, including for base model training (i.e. logistic regression, random forest), for all recourse experiments, and post-processing of results to produce metrics. The cluster contains:

- compute nodes with 28 cores of Xeon E5-2680 v4 (2.40GHz, 128GB RAM, and 200GB local SSD disk memory),
- compute nodes with 28 cores of Xeon Gold 6240 CPU units (2.60GHz, 192GB RAM, and 240GB local SSD), and
- compute nodes with 56 cores of Xeon E5-2680 v4 units (2.40GHz, 264GB RAM, and 30TB local disk).

We used nodes as they were available, with a range of 1-128 CPUs at a time.

¹so named for its shape when drawn on a whiteboard.